LANGMUIR

pubs.acs.org/Langmuir Article

Adenine Tagged Mn-Based Coordination Polymer for Conversion of Carbon Dioxide to Cyclic Carbonates under Atmospheric Pressure

Alehegn Eskemech, Rubi Bhakhar, Pritam Biswas, Anirban Karmakar, Venkata Krishnan,* and Rik Rani Koner*

Cite This: *Langmuir* 2025, 41, 19101−19110 Read Online

ACCESS | Metrics & More | Article Recommendations | Supporting Information

ABSTRACT: Natural processes collectively balance the global carbon cycle, effectively controlling atmospheric carbon dioxide (CO_2) levels. However, excessive CO_2 emissions due to industrialization and population growth have disrupted natural processes by increasing the atmospheric CO_2 concentration. To address this issue, CO_2 capture and conversion have been implemented. Metal−organic frameworks (MOFs)/coordination polymers (CPs) with bioligands, such as amino acids and nucleobases, are receiving much interest. However, bio-MOFs are not much reported due to the lack of control over their coordination with metal ions. In this work, we have developed an adenine-tagged Mn-CP with dominant basic sites, $[Mn(IPT^{2-})(Ade)(DMF)]_n$ (IPT^{2-} = isophthalate; Ade = adenine; DMF = *N*,*N*′-dimethylformamide). The analysis of isosteric heat (Q_{st}) of CO_2 adsorption supported the presence of strong interactions between CO_2 and Mn-CP. Mn-CP demonstrated moderate to outstanding performance in coupling CO_2 with smaller and larger epoxides at ambient pressure under neat conditions. The thermodynamic activation parameters indicate that Mn-CP operates through an associative mechanism ($\Delta S^{\ddagger} = -283.4$ J mol^{-1} K^{-1}), with a reduced kinetic barrier characterized by $\Delta H^{\ddagger}$ of 17.28 kJ mol^{-1} and E_a of 20.5 kJ mol^{-1}. The catalytic efficiency of Mn-CP was particularly notable in the coupling reaction of epichlorohydrin and CO_2, yielding 92% of the corresponding cyclic carbonate under atmospheric pressure.

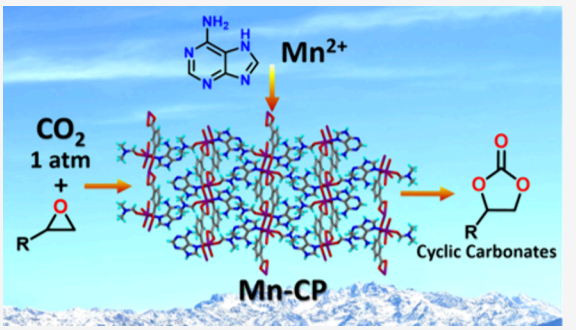

INTRODUCTION

Carbon dioxide (CO_2) is a crucial substrate in synthesizing carbohydrates through photosynthesis, thereby contributing to the balance of the carbon cycle.[1,2] Additionally, oceans serve as considerable carbon sinks, absorbing atmospheric CO_2 through dissolution and biological processes.[3,4] These natural processes balance the global carbon cycle and regulate atmospheric CO_2 levels. However, extensive CO_2 emissions caused by industrialization and population growth have disturbed this balance.[5,6] The excessive use of fossil fuels increases atmospheric CO_2 concentration, aggravating the threat of climate change (global warming) for the planet.[7] In response to this persistent concern, CO_2 capture, storage, and conversion have been practiced for the past few years.[8] In the area of conversion, CO_2 has been utilized to synthesize value-added chemicals, including fuels, fine chemicals, polymers, and pharmaceuticals.[8] One promising pathway for utilizing CO_2 involves reacting it with epoxides to form cyclic carbonates. This process has garnered significant interest because it provides a sustainable alternative to the traditional method of synthesizing cyclic carbonates.[9] Furthermore, the production of cyclic carbonates through reaction between CO_2 and epoxides is recognized for its complete atom efficiency and eco-friendly nature.[10,11] Cyclic carbonates are used in many industrial applications, including fuel additives,[11] polar solvents,[12] lithium battery electrolytes,[13] precursors for polycarbonate materials,[14] and pharmaceutical manufacturing.[15] Homogenous catalysts have been traditionally utilized to effectively synthesize cyclic carbonates with the cycloaddition of CO_2 and epoxides.[16] However, the use of homogeneous catalysts is limited due to issues such as catalyst deactivation, the need for high pressure and temperature, challenges in separating the catalyst from the product, and recyclability concerns. On the other hand, heterogeneous catalysts, such as metal complexes,[17−20] carbon-based catalysts,[21] silicas,[22] covalent organic frameworks[23−26] and metal−organic frameworks (MOFs)/coordination polymers (CPs)[27−29] are receiving a lot of regard, due to their effective catalytic activity, ease of separation from the product, and ability to be reused multiple times.

Received: February 22, 2025
Revised: June 2, 2025
Accepted: June 2, 2025
Published: July 14, 2025

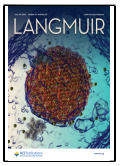

https://doi.org/10.1021/acs.langmuir.5c00906
Langmuir 2025, 41, 19101−19110

Among the various heterogeneous catalysts, MOFs/CPs, a class of hybrid materials comprising metal ions or clusters and organic ligands, have become the material of choice on account of their designability, tunability, and high adsorption capacity.[30] Since 2009, various classes of MOFs/CPs have been described as competent facilitators for transforming CO_2 and epoxides into cyclic carbonates.[31−34] However, most MOFs/CPs have required high pressure and/or high-temperature conditions for such reactions.[35−39] Meanwhile, several reports on single-ligand- and mixed-ligand-based MOFs/CPs have demonstrated high activity under ambient conditions.[40−44] On the other hand, MOFs/CPs effective under ambient conditions often require longer reaction times up to 48 h, limiting their practical applicability.[45] MOFs/CPs with biologically derived linkers have been extensively explored in areas such as biomedicine and sensing[46,47] but rarely for CO_2 conversion reactions.[48] For instance, various porous and nonporous adenine-based MOFs/CPs with diverse topologies and structure have been studied for applications like drug delivery, sensors, and gas adsorption.[47−49] Nevertheless, only a handful of reports have shown adenine-based MOFs/CPs being used for converting CO_2 to cyclic carbonates under either challenging or mild conditions.[48,50] Compared to other classes of MOFs/CPs, those incorporating nucleobases (e.g., adenine) are less detailed in the literature due to challenges in controlling their coordination modes with metal ions and their intrinsic lack of symmetry, which constrains packing in crystalline materials.[46,48,51] To address these challenges, carboxylic-acid-based ligands have been utilized in combination with adenine to construct metal-carboxylate-adenine MOFs/CPs. However, this approach remains more challenging than using synthetic nonbiological ligands.[46] Adenine-tagged MOFs/CPs composed of Cd(II), Zn(II), Cu(II), and Co, incorporating adenine and additional carboxylate ligands, are predominant in the literature.[48,49,52] However, Ni(II)[53] and Mn(II)[54]-based MOFs/CPs utilizing adenine and/or carboxylate ligands are notably scarce. Thus, developing MOFs/CPs using less-expensive, commercially available linkers featuring multiple potential sites and accessible noncovalent interaction sites (including hydrogen bonds) is paramount for effective CO_2 conversion under mild reaction conditions. Here, we developed a novel adenine tagged Mn-CP $[Mn(IPT^{2-})(Ade)(DMF)]_n$ (IPT^{2-} = isophthalate; Ade = adenine; DMF = *N*,*N*′-dimethylformamide) constructed from Mn(II), adenine, and isophthalic acid under solvothermal conditions. The Mn-CP exhibits dominant basic sites, crucial for activating the CO_2 molecules. The framework of Mn-CP is decorated with a free $-NH_2$/NH group, a potential basic site. Moreover, the computation of isosteric heat (Q_{st}) of CO_2 adsorption reveals a significant affinity between CO_2 and Mn-CP. Thus, Mn-CP was employed to synthesize various cyclic carbonates from CO_2 and epoxides under ambient pressure and mild temperature without further solvents. The free amine decorated Mn-CP endowed moderate to outstanding catalytic efficacy in the fixation of CO_2 with smaller and larger epoxides. The yield of cyclic carbonate achieved was as high as 92% during the coupling of CO_2 and epichlorohydrin.

EXPERIMENTAL SECTION

Synthesis of Mn-CP. Mn-CP was prepared through a solvothermal method. Particularly, 0.37 mmol of adenine (Ade) and 0.37 mmol of isophthalic acid (IPT) were dissolved in DMF (4 mL) separately, while 0.37 mmol of $Mn(CH_3COO)_2.4H_2O$ was dissolved in water (4 mL). Sonication and heating were used to dissolve the adenine completely. Each solution was poured into a 15-mL vial and maintained in an oven at 80 °C. After 4 days, pale pink crystals were obtained. The CP was collected from the mother liquor and rinsed with ethanol. Then, the collected crystal of Mn-CP was dried in an oven at 100 °C (yield: 80% with respect to Ade). Elemental analysis of $C_{16}H_{16}MnN_6O_5$ (MW = 427.29): Found: C 44.58; H, 4.21; N, 19.19%; calcd: 44.98; H, 3.77; N, 19.67%. FTIR (cm^{-1}): 3386, 3310, 1664, 1590, 1541, 145, 1395, 1300, 1221, 1106, 954, 901, 824, 828, 866, 746, 718, 676, 644, 521, 416.

Cycloaddition of CO_2 and Epoxides. The cycloaddition reaction of epoxide and CO_2 was executed under an atmospheric pressure. Specifically, a round-bottom flask (RBF) was loaded with epoxide (10 mmol), co-catalyst tetrabutylammonium bromide (TBAB) (0.62 mol %), and the catalyst, Mn-CP (varying amounts). The RBF was then attached to a condenser and exposed to a vacuum pump. The CO_2 gas was supplied to the reaction mixture via a balloon, and the CO_2 balloon was connected to the condenser. Then, the reaction was performed at 70 °C (24 h) accompanied by vigorous stirring at 600 rpm. Once the reaction was accomplished, the CO_2 line was turned off and allowed to return to ambient temperature. The Mn-CP was isolated from the product mixture using ethyl acetate via centrifugation. The product formed from epichlorohydrin was obtained via a rotavapor, whereas the product of phenyl glycidyl ether was obtained via pure hexane (HPLC) washing. Other epoxide products were isolated via column chromatography, using distilled hexane and ethyl acetate. The purity of the products was verified using ^1H and ^{13}C NMR (Supporting Information, Figures S34 and S45).

RESULTS AND DISCUSSION

Single-Crystal Analysis. Adenine's abundance of heteroatoms makes it well-suited for providing multiple coordination sites. However, adenine's intrinsically low symmetry and limited molecular length pose challenges when constructing MOFs/CPs using adenine as a single ligand.[46] In this context, isophthalic acid's high symmetry and angular geometry contribute significantly to the formation of robust frameworks. The symmetry of isophthalic acid complements adenine's flexible coordination sites effectively. Moreover, adenine offers unique advantages due to its multiple uncoordinated nitrogen sites, which function as Lewis basic sites that are essential for substrate activation. Also, due to the hydrogen bond donor−acceptor nature of adenine, it can activate the substrates. This synergy makes the combination of isophthalic acid and adenine particularly effective for the MOF/CP design. Thus, the adenine-tagged Mn-CP was synthesized using adenine (Ade) and isophthalic acid (IPT) (Scheme 1) under solvothermal conditions, as outlined in the Experimental Section.

The crystal structure analysis of Mn-CP, $[Mn(IPT^{2-})(Ade)(DMF)]_n$ (IPT^{2-} = isophthalate; Ade = adenine; DMF = *N*,*N*′-dimethylformamide), revealed its crystallization in the monoclinic $P2_1/n$ space group. The asymmetric unit entails one Mn(II) center, one isophthalate (IPT^{2-}), one adenine

Scheme 1. Synthesis Scheme of Mn-CP

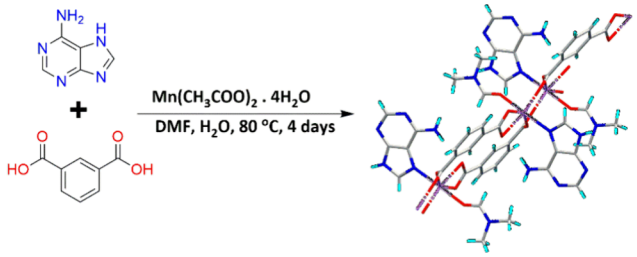

https://doi.org/10.1021/acs.langmuir.5c00906
Langmuir 2025, 41, 19101−19110

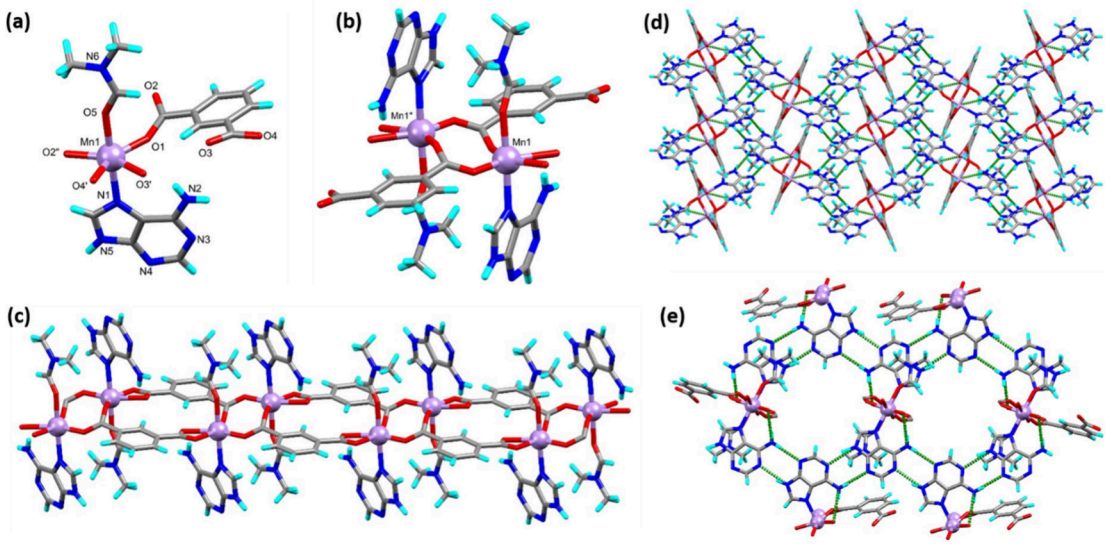

Figure 1. (a) Asymmetric unit of Mn-CP with partial atom labeling [symmetry code: ′ = 1 − *x*, 1 − *y*, 1 − *z*; ′′ = 1 − *x*, 1 − *y*, 2 − *z*], (b) coordination sphere around dinuclear $[Mn_2(IPT^{2-})_2]$ secondary building unit (SBU) [symmetry code: ′′ = 1 − *x*, 1 − *y*, 2 − *z*], (c) one-dimensional (1D) double chain network of Mn-CP presented in ball−stick; (d) hydrogen-bonded zig-zag two-dimensional assembly in Mn-CP and (e) cyclic hydrogen bonded network formed by the hydrogen bonding interactions between neighboring Ade molecules. Color code; Mn (violet), N (blue), O (red), C (gray), and H (cyan).

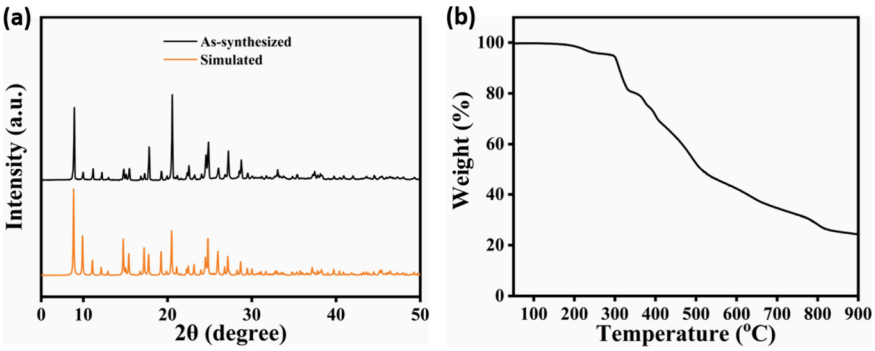

Figure 2. (a) PXRD patterns of simulated and as-synthesized Mn-CP. (b) TGA of Mn-CP.

(Ade), and one coordinated DMF (Figure 1a). Symmetry expansion exposes Mn-CP as a one-dimensional (1D) double-chain framework. Within this framework, the IPT^{2-} ligand coordinates simultaneously to three Mn(II) ions via carboxylate groups, acting as bridging bidentate and chelate monodentate donors, while the Ade ligand coordinates to one Mn(II) center via a nitrogen group, and the remaining amine and N do not coordinate to the metal center, participating only in hydrogen bonding interactions. The Mn(II) ions adopt a distorted octahedral geometry, with Mn1 occupied by four carboxylate-O atoms from three IPT^{2-} ligands in equatorial positions and the remaining axial positions filled by one N atom from an Ade ligand and one O atom from a DMF. The crystal data and structure refinement detail are tabulated in Table S1. In Mn-CP, Mn−O and Mn−N bond lengths range from 2.082(2)−2.273(2) Å and 2.294(2) Å, respectively, with bond angles ∠O−Mn−O and ∠O−Mn−N with ranges of 58.07(7)°−150.84° and 88.28(9)°−177.20(10)°, respectively (Table S2).

Within the framework of Mn-CP, two Mn(II) ions are bridged by two IPT^{2-} ligands, forming a $[Mn_2(IPT^{2-})_2]$ secondary building unit (SBU) (Figure 1b), with a Mn1··· Mn1′ distance of 4.165(7) Å. These dinuclear $[Mn_2(IPT^{2-})_2]$ SBUs connect via IPT^{2-} ligands to create a 1D double-chain structure (Figure 1c). These 1D structures further hydrogen-bond with each other via uncoordinated amine and N of Ade ligands through N2−H2A···N4 and N5−H5N···N3 interactions, forming a *zigzag* two-dimensional hydrogen-bonded assembly (Figure 1d). Moreover, these neighboring Ade ligands belonging to the 1D networks were connected to form a ring $R_2^2(8)$ type hydrogen-bonded cyclic network, as represented in Figure 1e. Additionally, N−H···O hydrogen bonding interaction (e.g., N2−H2B···O3) between carboxylated-O of IPT^{2-} ligands and free NH_2− groups of Ade are observed (Figure S1). Furthermore, various C−H···O interactions between the C−H of the Ade ligand and carboxylate-O contribute to stabilizing this 3D framework. All hydrogen-bond distances and angles are listed in Table S3.

Physical Characterizations. The crystallinity and phase purity of the bulk synthesized Mn-CP were inspected via powder X-ray diffraction (PXRD). The simulated and experimental PXRD data aligned closely with each other (Figure 2a), ensuring the crystalline purity of the bulk Mn-CP. Fourier transform infrared (FTIR) spectroscopy (Figure S2) was employed to verify the existence of different functionalities. The double peak observed at 3386 cm^{-1} and 3310 cm^{-1}

https://doi.org/10.1021/acs.langmuir.5c00906
Langmuir 2025, 41, 19101−19110

correlates to symmetrical and asymmetrical vibrations of the free $-NH_2$ functional group.[50] Additionally, 1664 cm^{-1} is associated with the C═O of DMF.[55] Furthermore, peaks detected at 1590 cm^{-1} and 1395 cm^{-1} are associated with the asymmetric and symmetric stretching of the O−C−O group from IPT, respectively.[56] Additionally, the Raman spectrum of Mn-CP is primarily characterized by vibrations associated with its organic ligands (Figure S3). The 600−1000 cm^{-1} bands correspond to the out-of-plane bending vibrations of the Ade and IPT^{2-} rings.[57] The peaks at 722, 832, 867, and 922 cm^{-1} are linked to C−H out-of-plane bending. The region between 1100 cm^{-1} and 1300 cm^{-1} is dominated by C−N stretching modes.[57] A peak at 1461 cm^{-1} is given to the symmetric stretching of the O−C−O group, while the peak at 1547 cm^{-1} corresponds to its asymmetric stretching.[58] Furthermore, peaks at 1003 and 1610 cm^{-1} are assigned to the symmetric and asymmetric stretching of the C═C bonds in the benzene ring, respectively.[58] To understand the thermal properties of this CP, thermogravimetric analysis (TGA) was conducted from ambient temperature to 900 °C under a N_2 environment (Figure 2b). As shown in Figure 2b, TGA of Mn-CP indicates a weight loss of 17.78% (cal. 17.08%) within the temperature range of up to 330 °C due to the dissociation of coordinated DMF.[59] Beyond this temperature threshold, continuous weight loss (Figure 2b) indicates breakage of the underlying CP structure.

The chemical composition of Mn-CP was established by using X-ray photoelectron spectroscopy (XPS). The XPS survey (Figure S4) of Mn-CP discloses the presence of C, O, N and Mn. In Figure 3a, the deconvolution of the C 1s peak

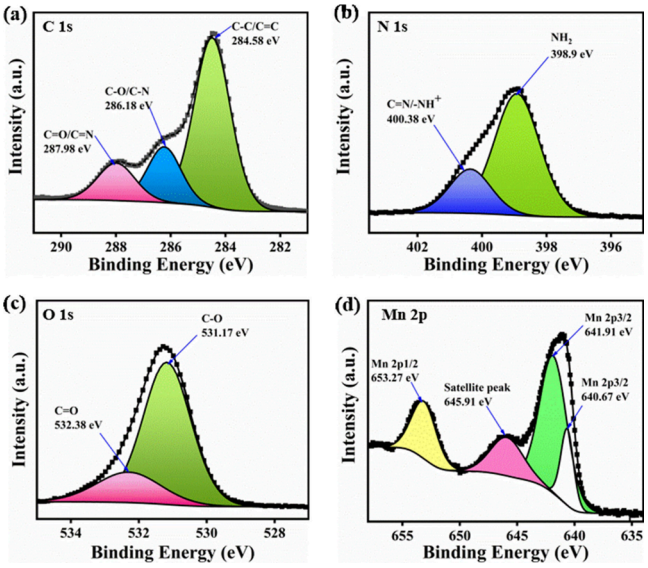

Figure 3. XPS spectra of (a) C 1s, (b) N 1s , (c) O 1s and (d) Mn 2p for Mn-CP.

reveals three distinct peaks at 284.58, 286.18, and 287.98 eV attributed to C−C/C═C, C−O/C−N, and C═O/C═N bonds, respectively.[60] Further deconvolution of N 1s spectra (Figure 3b) at 398.90 eV provides information on the presence of the NH_2 group, while the peak at 400.38 eV corresponds to the C═N/$-NH^+$.[54,61] The deconvolution of the O 1s spectra (Figure 3c) of Mn-CP revealed two distinct peaks at 531.17 and 532.38 eV, signifying the presence of C−O and C═O bonds, respectively.[62] The Mn 2p spectrum is deconvoluted into four characteristic peaks (Figure 3d). The peaks at 640.67 and 653.27 eV are given to Mn $2p_{3/2}$ and Mn $2p_{1/2}$, respectively. The peak at 641.91 eV is ascribed to Mn $2p_{3/2}$ spin−orbit coupling. Additionally, the peak at 645.91 eV is linked with the satellite peak, indicating a Mn(II) species.[63−65]

The CO_2 adsorption properties of this Mn-CP were estimated at 273 and 298 K, which displayed reasonable CO_2 adsorption properties. CO_2 uptake of Mn-CP was found to be 0.26 and 0.18 mmol g^{-1} at 273 and 298 K, respectively (Figure S5). In addition, the Brunauer−Emmett−Teller (BET) surface area was determined using CO_2 adsorption−desorption isotherms at 273 K and was found to be 14 m^2 g^{-1}, indicating that the material lacks porosity. Freundlich−Langmuir equations (eqs S1 and S2) and the Clausius−Clapeyron equation (eq S3) were employed to compute the isosteric heat (Q_{st}) of CO_2 adsorption in Mn-CP. This was achieved by initially fitting CO_2 adsorption isotherms at 273 and 293 K (Figures S6 and S7). The Q_{st} value sharply decreases from 46.5 kJ mol^{-1} to 10.5 kJ mol^{-1} with the loading amount (Figure S8). This higher Q_{st} value at lower loading is accredited to the strong interaction among the free NH_2 and N in the Mn-CP framework and CO_2.[66] The decrease in the Q_{st} value at higher loads and pressures ensures the occupation of the available active sites. The availability and strength of acidic and basic sites in Mn-CP were examined by NH_3 and CO_2 temperature-programmed desorption (TPD) methods. Generally, the acid and base strengths of the catalyst can be classified into three distinct regions: weak, moderate, and strong acidic/basic sites, corresponding to the temperature ranges of 50−200 °C, 200−400 °C, and 400−600 °C, respectively.[67,68] The CO_2-TPD analysis (Figure S9, Table S4) revealed the presence of medium basic sites in the Mn-CP. The medium basic sites were shown by peaks at 298 °C (0.169 mmol g^{-1}) and 340 °C (1.217 mmol g^{-1}). Similarly, NH_3-TPD analysis (Figure S10, Table S4) reveals the presence of medium acidic sites in Mn-CP, with peaks at 283 °C (0.169 mmol g^{-1}) and 337 °C (0.951 mmol g^{-1}). Thus, this Mn-CP consists of medium total basic (1.386 mmol g^{-1}) sites and acidic (1.12 mmol g^{-1}) sites, essential for the interaction of epoxide and CO_2.[69,70]

Catalytic Activity Studies. The acidic and basic sites are crucial for the cycloaddition reaction of CO_2 with epoxides.[71] Based on the features of both basic and acidic sites of Mn-CP, we conducted the CO_2 conversion reaction with epichlorohydrin (ECH) (2-(chloromethyl)oxirane) as a representative substrate. The reaction was operated at atmospheric pressure and under neat conditions. The optimal operating conditions of Mn-CP were optimized by using a fixed amount of ECH (10 mmol) and tetrabutylammonium bromide (TBAB) (0.062 mmol) while varying the Mn-CP loading, reaction temperature, and time. The findings are listed in Figure 4. The yield of 4-(chloromethyl)-1,3-dioxolan-2-one was 78%, with a Mn-CP loading of 40 mg (0.94 mol %). Furthermore, increasing the catalyst amount from 40 mg (0.94 mol %) to 60 mg (1.40 mol %) enhanced the yield of the product to 83%. The highest yield of 4-(chloromethyl)-1,3-dioxolan-2-one (92%) was achieved with a catalyst loading of 80 mg (1.87 mol %). However, further enhancing the catalyst amount (100 mg (2.34 mol %), induced a minor decline in the yield of the product (82%)(Figure 4a). This could be ascribed to the agglomeration of Mn-CP catalyst.[72] The temperature effect (Figure 4b) on the reaction of CO_2 with ECH was studied from 40 to 70 °C. As shown in Figure 4b, the yield of the

https://doi.org/10.1021/acs.langmuir.5c00906
Langmuir 2025, 41, 19101−19110

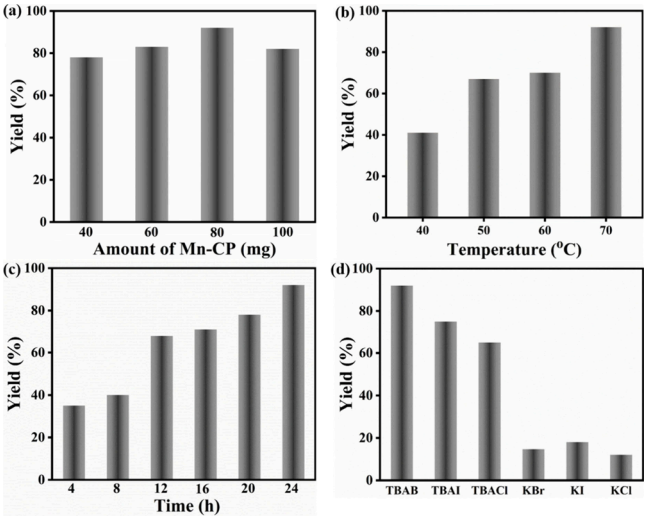

Figure 4. Optimization of parameters for catalytic reaction of CO_2 and cyclic carbonates: (a) Mn-CP loading (reaction conditions: 10 mmol epichlorohydrin, 0.62 mol % TBAB, balloon CO_2, 70 °C, 24 h), (b) reaction temperature (conditions: 80 mg (1.87 mol %) Mn-CP, 10 mmol ECH, 0.62 mol % TBAB, balloon CO_2, 24 h), (c) reaction time (conditions: 1.87 mol % Mn-CP, 10 mmol ECH, 0.62 mol % TBAB, balloon CO_2, 70 °C, and (d) co-catalyst effect (reaction conditions: 10 mmol ECH, 0.62 mol % TBAI, TBACl, KBr, KI, and KCl; 1.87 mol % Mn-CP, 70 °C, balloon CO_2, 24 h).

product was enhanced with increasing temperature, and a maximum yield was obtained at 70 °C. Reaction time is another crucial parameter for this reaction. Hence, the reaction time varied from 4 to 24 h, while other reaction parameters remained constant (1.87 mol % of catalyst loading, 70 °C, 0.62 mol % of TBAB, atmospheric CO_2 pressure) (Figure 4c). The investigation of the time-dependent experiment revealed that the maximum yield was obtained at 24 h of reaction. The optimization process revealed that Mn-CP was notably effective in the CO_2 reaction with ECH, using 1.87 mol % of Mn-CP at 70 °C for 24 h under ambient pressure.

Furthermore, we investigated the effect of various co-catalysts including tetrabutylammonium iodide (TBAI), tetrabutylammonium chloride (TBACl), and potassium halides (KI, KBr, and KCl), in addition to TBAB in the reaction of CO_2 and ECH with optimized settings (Figure 4d). As depicted in Figure 4d, the TBAB showed better co-catalytic activity than TBAI and TBACl. This may be ascribed to the better nucleophilicity of bromide than chloride. However, the co-catalytic performance of TBAI was found to be slightly less than that of TBAB due to the large size of the I^- ion. On the other hand, all the potassium halides (KCl, KBr, and KI) failed to enhance the catalytic activity of Mn-CP. This might result from the competition of the K^+ ion and CO_2 for the active sites. This competition hampers the adsorption and activation of CO_2 by basic sites, thereby reducing catalytic activity.[68]

While investigating the performance of the reaction with individual catalysts (Mn-CP, IPT, Ade, $Mn(CH_3COO)_2 \cdot 4H_2O$, mixture of the precursors of Mn-CP and TBAB), it was noticed that individual components exhibited lower efficiency, compared to the Mn-CP/TBAB system, suggesting synergistic effects of Mn-CP and TBAB boosted the cycloaddition reaction (Figure S11, Table S5). The catalytic activity of Mn-CP was evaluated without any co-catalyst, which displayed moderate activity with a yield of 33% for the corresponding cyclic carbonate of ECH (4-(chloromethyl)-1,3-dioxolan-2-one) (Table S5, entry 1). Meanwhile, IPT exhibited the lowest catalytic activity (4%) (Table S5, enrty2), while Ade showed moderate catalytic activity (37%) (Table S5, entry 3). Also, the formation of 4-(chloromethyl)-1,3-dioxolan-2-one was noticed with a 26% yield in the presence of Mn-$(CH_3COO)_2 \cdot 4H_2O$) as a catalyst (Table S5, entry 4). Whereas the physical mixture of the precursors of Mn-CP yielded only 9% of the product (Table S5, entry 5). When TBAB was employed only without the Mn-CP, the yield of the product was 41% (Table S5, entry 6). Integration of Mn-CP with TBAB resulted in a noteworthy increase in yield, reaching 92% for the corresponding cyclic carbonate of ECH (Table S5, entry 7). This synergistic effect suggests that the joint action of Mn-CP and TBAB boosts the catalytic activity and enhances the yield of the target product.

The catalytic efficacy of Mn-CP in the cycloaddition reaction of CO_2 with epichlorohydrin (ECH) was compared with those of previously reported adenine-tagged MOFs/CPs (Table S6). The literature shows that the number of adenine-based MOFs/CPs explored for this purpose remains limited. This Mn-CP offers more favorable operating conditions and maintains comparable catalytic efficiency. For instance, some adenine-based MOFs demonstrated high catalytic activity. However, the required CO_2 pressure was found to be high.[50,54] Furthermore, while comparing Mn-CP with various other reported Mn-based MOFs/Mn-CPs (Table S6), it becomes clear that some MOFs/CPs can catalyze this reaction at atmospheric pressure with longer reaction times. Thus, Mn-CP has demonstrated the ability to facilitate CO_2 fixation reactions at atmospheric pressure and mild temperatures, positioning it as a promising candidate.

Substrate Scope. The CO_2 fixation reaction was not only limited to coupling with ECH, it was also conducted with various other substrates, such as butyl glycidyl ether, *tert*-butyl glycidyl ether, allyl glycidyl ether, styrene oxide, and phenyl glycidyl ether under optimal working conditions (Table 1). In all substrate scope studies, the isolated cyclic carbonate yields were determined and ^1H and ^{13}C NMR confirmed the purity of each cyclic carbonate. As shown in Table 1, this Mn-CP efficiently transforms CO_2 and epoxides into particular cyclic carbonates. However, the yield of cyclic carbonate varied from one substrate to another. For example, epichlorohydrin and butyl glycidyl ether were converted to their corresponding cyclic products in 92% and 89% yields, respectively. The higher conversion of epichlorohydrin and butyl glycidyl ether might be attributed to their ability to interact effectively with the active sites of the catalyst.[73] While *tert*-butyl glycidyl ether and allyl glycidyl ether presented 75% and 77% yields for the corresponding cyclic carbonates, respectively. Furthermore, the catalytic activity was studied for phenyl glycidyl ether, resulting in an 80% yield of its corresponding cyclic product. The higher yield for the conversion of phenyl glycidyl ether might be due to the $\pi-\pi$ interaction between the phenyl ring of phenyl glycidyl ether and the aromatic rings of the Mn-CP, as observed in other reported MOFs/CPs as well.[74] Among the tested epoxides, 1,2-epoxydodecane exhibits a yield (29%) lower than that of other epoxides. This reduced conversion is primarily attributed to the longer alkyl chain, which exerts an electron-donating effect (inductive effect), thereby decreasing the electrophilicity of the epoxide.[75] Additionally, the high viscosity of 1,2-epoxydodecane poses a solubility challenge for tetrabutylammonium bromide(TBAB),[76,77] further contribu-

https://doi.org/10.1021/acs.langmuir.5c00906
Langmuir 2025, 41, 19101−19110

Table 1. Mn-CP Catalyzed Formation of Different Cyclic Carbonates[a]

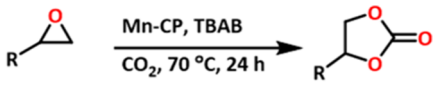

Entry	Reactants	Products	Yield (%)	TON	TOF (h^{-1})
1.		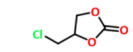	92	49	2.04
2.	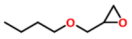	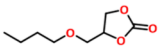	89	48	2.00
3.	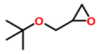	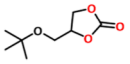	75	40	1.67
4.	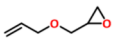	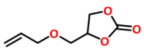	77	41	1.71
5.	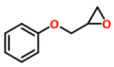	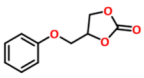	80	42	1.75
6.	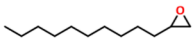	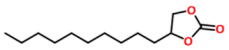	29	15	0.63

[a]Conditions: 1.87 mol % Mn-CP, 0.62 mol % TBAB, 10 mmol epoxide, 70 °C, 24 h, balloon CO_2. Yield was determined using the stoichiometric ratio. Turnover number (TON) = mmol of product/mmol of catalyst, Turnover frequency (TOF) = TON/time (h).

ting to the lower conversion of 1,2-epoxydodecane relative to other cyclic carbonates. In contrast, as can be seen from Table 1 (entries 1−5), epoxides with electron-withdrawing groups, such as chloro- or alkoxy- substituents at the alpha positions enhance the electrophilicity of the epoxide,[78] and are converted to corresponding cyclic carbonates in high yields.

Reaction Kinetics, Thermodynamics, and Mechanism. The kinetic and thermodynamic parameters for the chemical fixation of CO_2 with ECH, catalyzed by Mn-CP, were analyzed by conducting the reaction at 50, 60, and 70 °C. The kinetics of the reaction between CO_2 and ECH were studied by monitoring the concentration of ECH at different time intervals. The kinetics were evaluated by plotting the concentration of ECH against time (eq S4). A semilogarithmic plot (Figures S12−S14) confirmed that the reaction followed first-order kinetics. The rate constants for the reaction were determined from this plot and found to be 2.63×10^{-5} s^{-1}, 2.27×10^{-5} s^{-1}, and 1.67×10^{-5} s^{-1} at temperatures of 70, 60, and 50 °C, respectively. These results show the temperature-dependent nature of the catalytic process, with the reaction rate decreasing as the temperature lowers. Thermodynamic activation parameters,[68,79] including enthalpy ($\Delta H^{\ddagger}$) and entropy ($\Delta S^{\ddagger}$), were achieved from Eyring plots (eq S5, Figure S15). The values for $\Delta H^{\ddagger}$ and $\Delta S^{\ddagger}$ were 17.28 kJ $mol^{-1}$and −283.40 ± 5.32 J mol^{-1} K^{-1}, respectively. The lower $\Delta H^{\ddagger}$ value for Mn-CP (17.28 kJ mol^{-1}), compared to previously reported MOFs such as UOW-1 (23.6 kJ mol^{-1})[79] and Zn-MOF (29.3 ± 3.75 kJ mol^{-1})[68] suggests a lower kinetic barrier for Mn-CP in the coupling of CO_2 with ECH. The negative $\Delta S^{\ddagger}$ values indicate an associative mechanism similar to that observed with other MOFs.[68,79] The activation energy (E_a)[68,80] for the formation of 4-(chloromethyl)-1,3-dioxolan-2-one catalyzed by Mn-CP was 20.5 kJ mol^{-1}, indicating a moderate energy barrier for the CO_2 fixation reaction (eq S6, Figure S16). The Gibbs free energy ($\Delta G^{\ddagger}$) was computed from the fundamental thermodynamics equation (eq S7).[79] The values were 108.86 ± 2.1, 111.70 ± 2.35, and 114.53 ± 2.42 kJ mol^{-1} at temperatures of 50, 60, and 70 °C, respectively. The $\Delta G^{\ddagger}$ of the reactions increases with the temperature (Figure S17), again indicating a temperature-dependent reaction.

Based on our results and previous reports,[68,81−85] we propose the catalytic cycle for Mn-CP for the formation of cyclic carbonates through the reaction of CO_2 and epoxide, as depicted below (see Scheme 2). Numerous studies have shown that the Lewis basic and/or acid sites significantly impact the activation of substrates including epoxides and CO_2. In Mn-CP, the Mn(II) center is coordinatively saturated, as confirmed by SCXRD. Thus, substrate activation is primarily governed by Lewis basic sites and dispersive interactions, including hydrogen bonding.[81,83] In the initial step, the epoxides are activated through hydrogen bonding with the free $-NH_2$ group of adenine in Mn-CP (i) and dispersive interactions. Meanwhile, the interaction between CO_2 and the CP framework is governed by dispersive interactions, allowing CO_2 to interact weakly with the CP surfaces. Additionally, the nitrogen atoms in NH_2 groups and other uncoordinated nitrogen atoms within the adenine moieties of Mn-CP act as Lewis basic sites, promoting CO_2 adsorption. The Br^- from TBAB undergoes nucleophilic attack at the carbon of the epoxide from the less-substituted side to generate a haloalkoxide ((ii) and (iii)). Meanwhile, the NH_2/N moieties of adenine activate CO_2 molecules by forming a carbamate intermediate (iii). The haloalkoxide's nucleophilic attack on the carbamate intermediate causes the generation of the alkyl carboxylate (iv). At the end, ring closure (iv) gives cyclic carbonate (v), simultaneously regenerating both Mn-CP and TBAB for the next reaction cycles.

Recyclability of Mn-CP. The recyclability of Mn-CP was examined under optimized conditions using ECH. After each cycle, Mn-CP was separated from the product via centrifugation, followed by ethyl acetate and ethanol washing until no product was detected. Then, the Mn-CP catalyst was dried and used again for the subsequent cycle. The results show that the Mn-CP demonstrated consistent performance over three cycles with no decrease in product yield (Figure 5a). However, there was a decrease in efficacy in the fourth (82%) and fifth cycles (71%), likely due to the loss of Mn-CP during the recycling process. The TON value (Table S7) in each cycle was determined and found to be almost the same in the first four cycles (around 49), except for a slight decrement in the fifth cycle (around 47). The lifetime of the Mn-CP catalyst was estimated from the cumulative TON and found to be 225. This indicates that the catalyst can facilitate approximately 225 turnovers over the course of five cycles before its activity significantly decreases. Despite this decrease in catalytic activity, Mn-CP maintained its structural robustness over the cycles. The stability and structural integrity of Mn-CP were further investigated using various techniques. The recycled Mn-CP's PXRD patterns (Figure 5b) indicated that the overall structure and crystallinity remained the same after catalysis. Additionally, the FTIR spectra (Figure 5c) of the recycled Mn-CP closely resembled those of the fresh CP, with no changes in the characteristic peaks. The Raman spectra (Figure S18) of the recovered Mn-CP also closely correspond with those of the as-synthesized Mn-CP, confirming Mn-CP's structural integrity

https://doi.org/10.1021/acs.langmuir.5c00906
Langmuir 2025, 41, 19101−19110

Scheme 2. Proposed Mechanism for Mn-CP Catalyzed Synthesis of Cyclic Carbonates from CO_2 and Epoxides

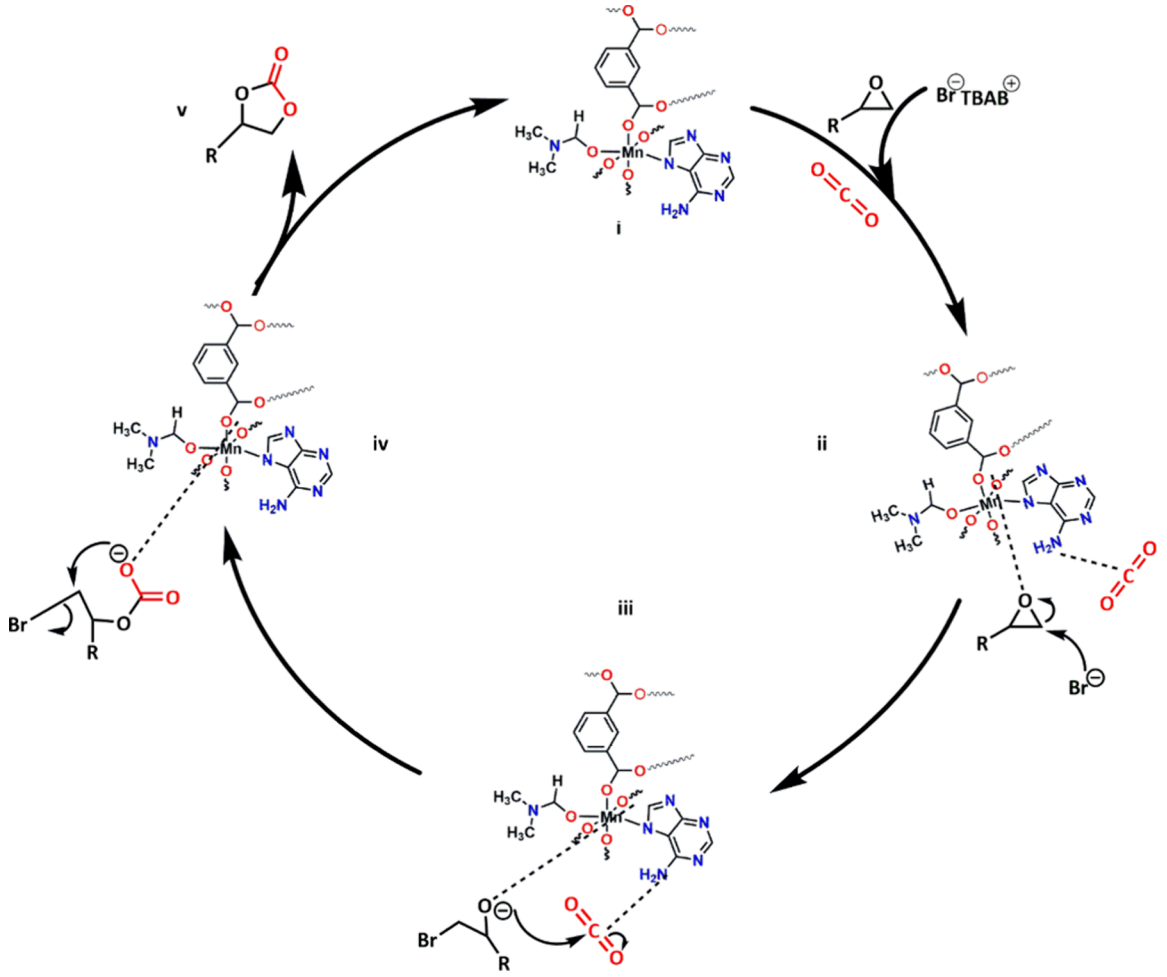

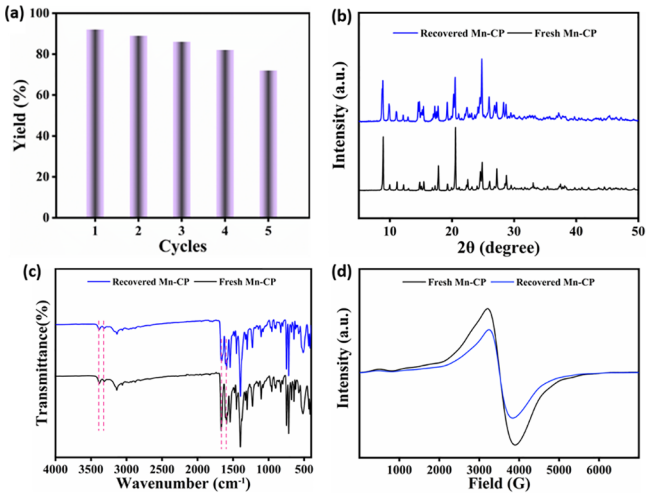

Figure 5. (a) Recyclability plot, (b) PXRD of fresh and recycled Mn-CP, (c) FTIR spectra of fresh and recycled Mn-CP, and (d) EPR spectra of fresh and recovered Mn-CP.

and stability following the catalytic process. The SEM images (Figure S19a and S19b) indicated no significant change in the morphology except for some agglomeration and/or particles sticking together (Figure S19b). The XPS analysis also supported the retention of the elemental composition of Mn-CP after the catalysis studies (Figure S20 and S21). We also conducted electron paramagnetic resonance (EPR) (Figure 5d) measurements to evaluate the coordination environment of the Mn-CP after catalysis. The g-factor for the as-synthesized Mn-CP (2.0038) and the recovered Mn-CP (2.0039) were found to be nearly identical. This similarity indicates that the coordination environment of the Mn centers remains stable throughout the catalytic process. The consistent g-factors suggest that the geometry and ligand arrangement around the metal ions are preserved, with no observable oxidation state or coordination number changes.[86] All of these results collectively confirm the heterogeneous nature of Mn-CP in the fixation of CO_2 with epoxides.

CONCLUSIONS

In this study, we have prepared a novel Mn-CP, $[Mn(IPT^{2-})(Ade)(DMF)]_n$ using the adenine (Ade)and isophthalic acid (IPT). As observed from SCXRD, Mn-CP contains uncoordinated nitrogen and free $-NH_2$ groups, essential basic sites for substrate activation. Although it exhibited low CO_2 uptake, the high isosteric heat of CO_2 adsorption confirms strong interactions between CO_2 molecules and the CP's basic sites. The Mn-CP/TBAB presented efficient activity in the solvent-free fixation of CO_2 with epoxides under ambient pressure and mild temperatures and exhibited moderate to high catalytic activity for smaller and larger epoxides. However, the integration of Mn-CP with KCl, KBr, and KI as co-catalysts significantly inhibited the catalytic activity of Mn-CP, likely

https://doi.org/10.1021/acs.langmuir.5c00906
Langmuir 2025, 41, 19101−19110

due to competition from potassium ions for the active sites. Kinetic analysis revealed that the reaction between ECH and CO_2, catalyzed by Mn-CP, follows first-order kinetics. The Mn-CP also displays a lower kinetic barrier ($\Delta H^{\ddagger}$ = 17.28 kJ mol^{-1}, E_a = 20.5 kJ mol^{-1}) and operates through an associative mechanism, as indicated by its thermodynamic activation parameters. Notably, Mn-CP's crystallinity and structural robustness were retained even after five cycles of CO_2 and ECH cycloaddition. Overall, this work highlights the potential of adenine-based Mn-CP as a promising catalyst for CO_2 fixation under mild temperatures and atmospheric pressure under neat conditions.

■ ASSOCIATED CONTENT

Supporting Information

The Supporting Information is available free of charge at https://pubs.acs.org/doi/10.1021/acs.langmuir.5c00906.

Chemicals and methods, crystallographic analysis, gas adsorption properties, TPD profile, isosteric heat of CO_2 adsorption (Q_{st}) analysis, kinetics and thermodynamic analysis, and NMR spectra of products (DOCX)

SCXRD data for Mn-CP with CCDC No. 2368573 (CIF)

■ AUTHOR INFORMATION

Corresponding Authors

Rik Rani Koner − *School of Mechanical and Materials Engineering, Indian Institute of Technology Mandi, Mandi 175075 Himachal Pradesh, India;* orcid.org/0000-0002-1600-5805; Email: rik@iitmandi.ac.in

Venkata Krishnan − *School of Chemical Sciences, Indian Institute of Technology Mandi, Mandi 175075 Himachal Pradesh, India;* orcid.org/0000-0002-4453-0914; Email: vkn@iitmandi.ac.in

Authors

Alehegn Eskemech − *School of Chemical Sciences, Indian Institute of Technology Mandi, Mandi 175075 Himachal Pradesh, India*

Rubi Bhakhar − *School of Chemical Sciences, Indian Institute of Technology Mandi, Mandi 175075 Himachal Pradesh, India*

Pritam Biswas − *School of Chemical Sciences, Indian Institute of Technology Mandi, Mandi 175075 Himachal Pradesh, India*

Anirban Karmakar − *Centro de Estudos de Engenharia Química, Instituto Superior de Engenharia de Lisboa, Instituto Politécnico de Lisboa, 1959-007 Lisboa, Portugal;* orcid.org/0000-0003-3047-2204

Complete contact information is available at: https://pubs.acs.org/10.1021/acs.langmuir.5c00906

Notes

The authors declare no competing financial interest.

■ ACKNOWLEDGMENTS

The authors gratefully acknowledge the Advanced Materials Research Center (AMRC) at IIT Mandi for providing access to their facilities. A.E. and R.B. thank the Ministry of Education, Government of India, for their respective doctoral fellowships.

■ REFERENCES

(1) Shi, J.; Jiang, Y.; Jiang, Z.; Wang, X.; Wang, X.; Zhang, S.; Han, P.; Yang, C. Enzymatic conversion of carbon dioxide. *Chem. Soc. Rev.* **2015**, *44* (17), 5981−6000.

(2) Olah, G. A.; Prakash, G. K.; Goeppert, A. Anthropogenic chemical carbon cycle for a sustainable future. *J. Am. Chem. Soc.* **2011**, *133* (33), 12881−12898.

(3) Raven, J. A.; Falkowski, P. G. Oceanic sinks for atmospheric CO_2. *Plant Cell Environ.* **1999**, *22* (6), 741−755.

(4) Gruber, N.; Bakker, D. C. E.; DeVries, T.; Gregor, L.; Hauck, J.; Landschuetzer, P.; McKinley, G. A.; Mueller, J. D. Trends and variability in the ocean carbon sink. *Nat. Rev. Earth Environ.* **2023**, *4* (2), 119−134.

(5) Yu, K. M. K.; Curcic, I.; Gabriel, J.; Tsang, S. C. E. Recent advances in CO_2 capture and utilization. *ChemSusChem* **2008**, *1* (11), 893−899.

(6) Mishra, A. K.; Agrawal, S. B.; Agrawal, M. *Rising Atmospheric Carbon Dioxide and Plant Responses: Current and Future Consequences*; Elsevier, 2019; pp 265−306.

(7) Gahlawat, I. N.; Lakra, P. Global Climate change and its effects. *Integr. J. Soc. Sci.* **2020**, *7* (1), 14−23.

(8) Alves, M.; Grignard, B.; Méreau, R.; Jerome, C.; Tassaing, T.; Detrembleur, C. Organocatalyzed coupling of carbon dioxide with epoxides for the synthesis of cyclic carbonates: catalyst design and mechanistic studies. *Catal. Sci. Technol.* **2017**, *7* (13), 2651−2684.

(9) Cokoja, M.; Wilhelm, M. E.; Anthofer, M. H.; Herrmann, W. A.; Kühn, F. E. Synthesis of Cyclic Carbonates from Epoxides and Carbon Dioxide by Using Organocatalysts. *ChemSusChem* **2015**, *8* (15), 2436−2454.

(10) Kiatkittipong, K.; Mohamad Shukri, M. A. A.; Kiatkittipong, W.; Lim, J. W.; Show, P. L.; Lam, M. K.; Assabumrungrat, S. Green pathway in utilizing CO_2 via cycloaddition reaction with epoxide—A mini review. *Processes* **2020**, *8* (5), 548.

(11) Guo, L. P.; Lamb, K. J.; North, M. Recent developments in organocatalysed transformations of epoxides and carbon dioxide into cyclic carbonates. *Green Chem.* **2021**, *23* (1), 77−118.

(12) Parker, H. L.; Sherwood, J.; Hunt, A. J.; Clark, J. H. Cyclic carbonates as green alternative solvents for the Heck reaction. *ACS Sustain. Chem. Eng.* **2014**, *2* (7), 1739−1742.

(13) Etacheri, V.; Marom, R.; Elazari, R.; Salitra, G.; Aurbach, D. Challenges in the development of advanced Li-ion batteries: a review. *Energy Environ. Sci.* **2011**, *4* (9), 3243−3262.

(14) Bobbink, F. D.; van Muyden, A. P.; Dyson, P. J. En route to CO_2 containing renewable materials: catalytic synthesis of polycarbonates and non-isocyanate polyhydroxyurethanes derived from cyclic carbonates. *Chem. Commun.* **2019**, *55* (10), 1360−1373.

(15) Martín, C.; Fiorani, G.; Kleij, A. W. Recent advances in the catalytic preparation of cyclic organic carbonates. *ACS Catal.* **2015**, *5* (2), 1353−1370.

(16) Dibenedetto, A.; Angelini, A.; Stufano, P. Use of carbon dioxide as feedstock for chemicals and fuels: homogeneous and heterogeneous catalysis. *J. Chem. Technol. Biotechnol.* **2014**, *89* (3), 334−353.

(17) Mihara, M.; Nakao, S.; Nakai, T.; Mizuno, T. Zinc Iodide-Metal Chloride-Organic Base: An Efficient Catalytic System for Synthesis of Cyclic Carbonates from Carbon Dioxide and Epoxides under Ambient Conditions. *Catalysts* **2023**, *13* (8), 1214.

(18) Qing, Y.; Liu, T.; Zhao, B.; Bao, X.; Yuan, D.; Yao, Y. Cycloaddition of di-substituted epoxides and CO_2 under ambient conditions catalysed by rare-earth poly (phenolate) complexes. *Inorg. Chem. Front.* **2022**, *9* (12), 2969−2979.

(19) Emelyanov, M. A.; Lisov, A. A.; Medvedev, M. G.; Maleev, V. I.; Larionov, V. A. Cobalt(III) Complexes as Bifunctional Hydrogen-Bond Donor Catalysts Featuring Halide Anions for Cyclic Carbonate Synthesis at Ambient Temperature and Pressure: A Mechanistic Insight. *Asian J. Org. Chem.* **2022**, *11* (5), e202100811.

(20) Emelyanov, M. A.; Stoletova, N. V.; Lisov, A. A.; Medvedev, M. G.; Smol'yakov, A. F.; Maleev, V. I.; Larionov, V. A. An octahedral cobalt(iii) complex based on cheap 1,2-phenylenediamine as a bifunctional metal-templated hydrogen bond donor catalyst for

fixation of CO_2 with epoxides under ambient conditions. *Inorg. Chem. Front.* **2021**, *8* (16), 3871−3884.
(21) Sahil; Gupta, N. Cyclic carbonates: Treasure of fine chemicals obtained from waste stream CO_2 over carbon-based heterogeneous catalysts. *Renew. Sustain. Energy Rev.* **2024**, *193*, 114297.
(22) Guan, R.; Zhang, X.; Chang, F.; Xue, N.; Yang, H. Incorporation of flexible ionic polymers into a Lewis acid-functionalized mesoporous silica for cooperative conversion of CO_2 to cyclic carbonates. *Chin. J. Catal.* **2019**, *40* (12), 1874−1883.
(23) Haque, N.; Biswas, S.; Ghosh, S.; Chowdhury, A. H.; Khan, A.; Islam, S. M. Zn(II)-embedded nanoporous covalent organic frameworks for catalytic conversion of CO_2 under solvent-free conditions. *ACS Appl. Nano Mater.* **2021**, *4* (8), 7663−7674.
(24) Luo, R.; Yang, Y.; Chen, K.; Liu, X.; Chen, M.; Xu, W.; Liu, B.; Ji, H.; Fang, Y. Tailored covalent organic frameworks for simultaneously capturing and converting CO_2 into cyclic carbonates. *J. Mater. Chem. A* **2021**, *9* (37), 20941−20956.
(25) Pang, Y.; Wang, B.; Gu, X.; Shen, H.; Yan, X.; Li, Y.; Chen, L. Hydroxy-Rich Covalent Organic Framework for the Efficient Catalysis of the Cycloaddition of CO_2. *Langmuir* **2023**, *39* (47), 16721−16730.
(26) Srinivasappa, P. M.; Hamzad, S.; Manjunath, H.; Samal, A. K.; Kumarswamy, Y. K.; Raghu, M. S.; Jadhav, A. H. Harnessing the Engineered 2D Triazine-Based Metal-Anchored Covalent-Organic Framework as a Catalyst for Selective Conversion of CO2 into Value-Added Products at Atmospheric Pressure. *ACS Sustain. Chem. Eng.* **2024**, *12* (25), 9428−9445.
(27) Pettinari, C.; Marchetti, F.; Mosca, N.; Tosi, G.; Drozdov, A. Application of metal- organic frameworks. *Polym. Int.* **2017**, *66* (6), 731−744.
(28) Furukawa, H.; Cordova, K. E.; O'Keeffe, M.; Yaghi, O. M. The chemistry and applications of metal-organic frameworks. *Science* **2013**, *341* (6149), 1230444.
(29) Hsieh, P.-F.; Law, Z. X.; Lin, C.-H.; Tsai, D.-H. Understanding Solvothermal Growth of Metal-Organic Framework Colloids for CO_2 Capture Applications. *Langmuir* **2022**, *38* (14), 4415−4424.
(30) Li, D.; Yadav, A.; Zhou, H.; Roy, K.; Thanasekaran, P.; Lee, C. Advances and Applications of Metal-Organic Frameworks (MOFs) in Emerging Technologies: A Comprehensive Review. *Global Chall.* **2024**, *8* (2), 2300244.
(31) Pal, T. K.; De, D.; Bharadwaj, P. K. Metal−organic frameworks for the chemical fixation of CO_2 into cyclic carbonates. *Coord. Chem. Rev.* **2020**, *408*, 213173.
(32) Beyzavi, M. H.; Stephenson, C. J.; Liu, Y.; Karagiaridi, O.; Hupp, J. T.; Farha, O. K. Metal-organic framework-based catalysts: chemical fixation of CO_2 with epoxides leading to cyclic organic carbonates. *Front. Energy Res.* **2015**, *2*, 63.
(33) Song, J.; Zhang, Z.; Hu, S.; Wu, T.; Jiang, T.; Han, B. MOF-5/n-Bu_4NBr: an efficient catalyst system for the synthesis of cyclic carbonates from epoxides and CO_2 under mild conditions. *Green Chem.* **2009**, *11* (7), 1031−1036.
(34) Li, Z.; Li, S.; Zhu, M.; Liu, Q.; Zhang, Y.; Wang, Y.; Wu, L.; Jiang, X. Interfacial Microenvironment-Regulated Coordinate Structures Dictate the Metal-Organic Framework Facet Orientation toward Efficient CO_2 Cycloaddition. *Langmuir* **2024**, *40* (48), 25518−25528.
(35) Guillerm, V.; Weseliński, Ł. J.; Belmabkhout, Y.; Cairns, A. J.; D'Elia, V.; Wojtas, Ł.; Adil, K.; Eddaoudi, M. Discovery and introduction of a (3,18)-connected net as an ideal blueprint for the design of metal−organic frameworks. *Nat. Chem.* **2014**, *6* (8), 673−680.
(36) Huang, X.; Chen, Y.; Lin, Z.; Ren, X.; Song, Y.; Xu, Z.; Dong, X.; Li, X.; Hu, C.; Wang, B. Zn-BTC MOFs with active metal sites synthesized via a structure-directing approach for highly efficient carbon conversion. *Chem. Commun.* **2014**, *50* (20), 2624−2627.
(37) Xiang, W.; Ren, J.; Chen, S.; Shen, C.; Chen, Y.; Zhang, M.; Liu, C. -j. The metal-organic framework UiO-66 with missing-linker defects: A highly active catalyst for carbon dioxide cycloaddition. *Appl. Energy* **2020**, *277*, 115560.
(38) Xue, Z.; Jiang, J.; Ma, M.-G.; Li, M.-F.; Mu, T. Gadolinium-Based Metal-Organic Framework as an Efficient and Heterogeneous Catalyst To Activate Epoxides for Cycloaddition of CO_2 and Alcoholysis. *ACS Sustain. Chem. Eng.* **2017**, *5* (3), 2623−2631.
(39) Xu, Z.; Zhao, Y.-Y.; Chen, L.; Zhu, C.-Y.; Li, P.; Gao, W.; Li, J.-Y.; Zhang, X.-M. Thermally activated bipyridyl-based Mn-MOFs with Lewis acid-base bifunctional sites for highly efficient catalytic cycloaddition of CO_2 with epoxides and Knoevenagel condensation reactions. *Dalton Trans.* **2023**, *52* (12), 3671−3681.
(40) Li, X.-Y.; Ma, L.-N.; Liu, Y.; Hou, L.; Wang, Y.-Y.; Zhu, Z. Honeycomb metal-organic framework with lewis acidic and basic bifunctional sites: selective adsorption and CO_2 catalytic fixation. *ACS Appl. Mater. Interfaces* **2018**, *10* (13), 10965−10973.
(41) Liu, S.; Gao, M.-L.; Zhang, Y.; Liu, L.; Han, Z.-B. Trifunctional Metal-Organic Framework Catalyst for CO_2 Conversion into Cyclic Carbonates. *Inorg. Chem.* **2021**, *60* (9), 6152−6156.
(42) Ma, R.; Qiao, C.; Xia, L.; Xia, Z.; Yang, Q.; Xu, Y.; Xie, G.; Chen, S.; Gao, S. Dynamic Metal-Iodide Bonds in a Tetracoordinated Cadmium-Based Metal-Organic Framework Boosting Efficient CO_2 Cycloaddition under Solvent-and Cocatalyst-Free Conditions. *Inorg. Chem.* **2022**, *61* (19), 7484−7496.
(43) Wang, L.; Qiao, W.; Liu, H.; Li, S.; Wu, J.; Hou, H. Synergistic Effects of Lewis Acid-Base Pair Sites-Hf-MOFs with Functional Groups as Distinguished Catalysts for the Cycloaddition of Epoxides with CO_2. *Inorg. Chem.* **2023**, *62* (9), 3817−3826.
(44) Bayer, U.; Werner, D.; Maichle-Mössmer, C.; Anwander, R. Effective and reversible carbon dioxide insertion into cerium pyrazolates. *Angew. Chem., Int. Ed.* **2020**, *59* (14), 5830−5836.
(45) Gao, W. Y.; Chen, Y.; Niu, Y.; Williams, K.; Cash, L.; Perez, P. J.; Wojtas, L.; Cai, J.; Chen, Y. S.; Ma, S. Crystal engineering of an nbo topology metal-organic framework for chemical fixation of CO_2 under ambient conditions. *Angew. Chem., Int. Ed.* **2014**, *53* (10), 2615−2619.
(46) Anderson, S. L.; Stylianou, K. C. Biologically derived metal organic frameworks. *Coord. Chem. Rev.* **2017**, *349*, 102−128.
(47) McKinlay, A. C.; Morris, R. E.; Horcajada, P.; Férey, G.; Gref, R.; Couvreur, P.; Serre, C. BioMOFs: metal-organic frameworks for biological and medical applications. *Angew. Chem., Int. Ed.* **2010**, *49* (36), 6260−6266.
(48) Gupta, R. K.; Riaz, M.; Ashafaq, M.; Gao, Z.-Y.; Varma, R. S.; Li, D.-C.; Cui, P.; Tung, C.-H.; Sun, D. Adenine-incorporated metal-organic frameworks. *Coord. Chem. Rev.* **2022**, *464*, 214558.
(49) Amo-Ochoa, P.; Zamora, F. Coordination polymers with nucleobases: From structural aspects to potential applications. *Coord. Chem. Rev.* **2014**, *276*, 34−58.
(50) Rachuri, Y.; Kurisingal, J. F.; Chitumalla, R. K.; Vuppala, S.; Gu, Y.; Jang, J.; Choe, Y.; Suresh, E.; Park, D.-W. Adenine-based Zn(II)/Cd(II) metal-organic frameworks as efficient heterogeneous catalysts for facile CO_2 fixation into cyclic carbonates: A DFT-supported study of the reaction mechanism. *Inorg. Chem.* **2019**, *58* (17), 11389−11403.
(51) Cai, H.; Huang, Y.-L.; Li, D. Biological metal-organic frameworks: Structures, host-guest chemistry and bio-applications. *Coord. Chem. Rev.* **2019**, *378*, 207−221.
(52) Zhang, M.; Gu, Z.-Y.; Bosch, M.; Perry, Z.; Zhou, H.-C. Biomimicry in metal-organic materials. *Coord. Chem. Rev.* **2015**, *293*, 327−356.
(53) Gładysiak, A.; Nguyen, T. N.; Anderson, S. L.; Boyd, P. G.; Palgrave, R. G.; Bacsa, J.; Smit, B.; Rosseinsky, M. J.; Stylianou, K. C. Shedding light on the protonation states and location of protonated N atoms of adenine in metal-organic frameworks. *Inorg. Chem.* **2018**, *57* (4), 1888−1900.
(54) Feng, C.; Qiao, S.; Guo, Y.; Xie, Y.; Zhang, L.; Akram, N.; Li, S.; Wang, J. Adenine-assisted synthesis of functionalized F-Mn-MOF-74 as an efficient catalyst with enhanced catalytic activity for the cycloaddition of carbon dioxide. *Colloids Surf. A: Physicochem. Eng. Asp.* **2020**, *597*, 124781.
(55) Sheta, S. M.; El-Sheikh, S. M.; Abd-Elzaher, M. M.; Ghanem, M. L.; Salem, S. R. A novel, fast, high sensitivity biosensor for supporting therapeutic decisions and onset actions for chest pain cases. *RSC Adv.* **2019**, *9* (35), 20463−20471.

https://doi.org/10.1021/acs.langmuir.5c00906
Langmuir 2025, 41, 19101−19110

(56) Maity, R.; Singh, H. D.; Yadav, A. K.; Chakraborty, D.; Vaidhyanathan, R. Water-stable Adenine-based MOFs with Polar Pores for Selective CO_2 Capture. *Chem.—Asian J.* **2019**, *14* (20), 3736−3741.
(57) Chen, S.; Li, X.; Dong, E.; Lv, H.; Yang, X.; Liu, R.; Liu, B. Intrinsic and Extrinsic Responses of ZIF-8 under High Pressure: A Combined Raman and X-ray Diffraction Investigation. *J. Phys. Chem. C* **2019**, *123* (49), 29693−29707.
(58) Prestipino, C.; Regli, L.; Vitillo, J. G.; Bonino, F.; Damin, A.; Lamberti, C.; Zecchina, A.; Solari, P. L.; Kongshaug, K. O.; Bordiga, S. Local Structure of Framework Cu(II) in HKUST-1 Metallorganic Framework: Spectroscopic Characterization upon Activation and Interaction with Adsorbates. *Chem. Mater.* **2006**, *18* (5), 1337−1346.
(59) Parsaei, M.; Akhbari, K.; Tylianakis, E.; Froudakis, G. E. Computational Simulation of a Three-Dimensional Mg-based Metal-Organic Framework as Nanoporous Anticancer Drug Carrier. *Cryst. Growth Des.* **2023**, *23* (11), 8396−8406.
(60) Wu, Y.; Song, X.; Li, S.; Zhang, J.; Yang, X.; Shen, P.; Gao, L.; Wei, R.; Zhang, J.; Xiao, G. 3D-monoclinic M-BTC MOF (M = Mn, Co, Ni) as highly efficient catalysts for chemical fixation of CO_2 into cyclic carbonates. *J. Ind. Eng. Chem.* **2018**, *58*, 296−303.
(61) Abbas, M.; Maceda, A. M.; Xiao, Z.; Zhou, H.-C.; Balkus, K. J. Transformation of a copper-based metal-organic polyhedron into a mixed linker MOF for CO_2 capture. *Dalton Trans.* **2023**, *52* (14), 4415−4422.
(62) Zheng, D.; Wen, H.; Sun, X.; Guan, X.; Zhang, J.; Tian, W.; Feng, H.; Wang, H.; Yao, Y. Ultrathin Mn Doped Ni-MOF Nanosheet Array for Highly Capacitive and Stable Asymmetric Supercapacitor. *Chem.—Eur. J.* **2020**, *26* (71), 17149−17155.
(63) Goswami, A.; Ghosh, D.; Pradhan, D.; Biradha, K. In Situ Grown Mn(II) MOF upon Nickel Foam Acts as a Robust Self-Supporting Bifunctional Electrode for Overall Water Splitting: A Bimetallic Synergistic Collaboration Strategy. *ACS Appl. Mater. Interfaces.* **2022**, *14* (26), 29722−29734.
(64) Hayashi, M.; Lee, D. T.; de Mello, M. D.; Boscoboinik, J. A.; Tsapatsis, M. ZIF-8 Membrane Permselectivity Modification by Manganese(II) Acetylacetonate Vapor Treatment. *Angew. Chem., Int. Ed.* **2021**, *60* (17), 9316−9320.
(65) Gu, R.-Y.; Liu, S.; Zhang, W.-C.; Li, L.-L.; Zhu, J.-B.; Chen, M.-R.; Zhou, H. A new Mn(II)-based metal-organic framework: synthesis, characterization, ferrimagnetic behavior and catalytic conversion of CO_2 to cyclic carbonates. *Inorg. Chim. Acta* **2024**, *565*, 121978.
(66) Sumida, K.; Rogow, D. L.; Mason, J. A.; McDonald, T. M.; Bloch, E. D.; Herm, Z. R.; Bae, T.-H.; Long, J. R. Carbon Dioxide Capture in Metal-Organic Frameworks. *Chem. Rev.* **2012**, *112* (2), 724−781.
(67) Chen, H.; Zhang, T.; Liu, S.; Lv, H.; Fan, L.; Zhang, X. Fluorine-Functionalized NbO-Type $\{Cu_2\}$-Organic Framework: Enhanced Catalytic Performance on the Cycloaddition Reaction of CO_2 with Epoxides and Deacetalization-Knoevenagel Condensation. *Inorg. Chem.* **2022**, *61* (30), 11949−11958.
(68) Eskemech, A.; Chand, H.; Karmakar, A.; Krishnan, V.; Koner, R. R. Zn-MOF as a Single Catalyst with Dual Lewis Acidic and Basic Reaction Sites for CO_2 Fixation. *Inorg. Chem.* **2024**, *63* (8), 3757−3768.
(69) Tapiador, J.; Garcia-Rojas, E.; Leo, P.; Martos, C.; Calleja, G.; Orcajo, G. Copper MOFs performance in the cycloaddition reaction of CO2 and epoxides. *Microporous and Mesoporous Materials* **2023**, *361*, 112741.
(70) Kim, J.; Kim, S.-N.; Jang, H.-G.; Seo, G.; Ahn, W.-S. CO_2 cycloaddition of styrene oxide over MOF catalysts. *Appl. Catal. A—Gen.* **2013**, *453*, 175−180.
(71) Wang, W.; Chen, W.; Yuan, W.; Xu, H. Q.; Liu, B. Hexagonal Cages and Lewis Acid-Base Sites in a Metal-Organic Framework for Synergistic CO_2 Capture and Conversion under Mild Conditions. *Inorg. Chem.* **2022**, *61* (45), 17937−17942.
(72) Melvin, A. C.; Reynolds, M. M. Systematic Exploration of a Catalytic Metal-Organic Framework/Polyurethane Composite for Medical Device Applications: Effects of MOF Particle Size, MOF Loading, and Polymer Concentration on Composite Material Activity. *Front. Phys.* **2022**, *10*, 880841.
(73) Wang, L.; Qiao, W.; Liu, H.; Li, S.; Wu, J.; Hou, H. Synergistic Effects of Lewis Acid-Base Pair Sites-Hf-MOFs with Functional Groups as Distinguished Catalysts for the Cycloaddition of Epoxides with CO_2. *Inorg. Chem.* **2023**, *62* (9), 3817−3826.
(74) Liang, L.; Liu, C.; Jiang, F.; Chen, Q.; Zhang, L.; Xue, H.; Jiang, H. L.; Qian, J.; Yuan, D.; Hong, M. Carbon dioxide capture and conversion by an acid-base resistant metal-organic framework. *Nat.Commun.* **2017**, *8* (1), 1233.
(75) Ganesan, V.; Yoon, S. Hyper-Cross-Linked Porous Porphyrin Aluminum(III)Tetracarbonylcobaltate as a Highly Active Heterogeneous Bimetallic Catalyst for the Ring-Expansion Carbonylation of Epoxides. *ACS Appl. Mater. Interfaces* **2019**, *11* (20), 18609−18616.
(76) Bai, D.; Nian, G.; Wang, G.; Wang, Z. Titanocene dichloride/KI: an efficient catalytic system for synthesis of cyclic carbonates from epoxides and CO_2. *Appl. Organomet. Chem.* **2013**, *27* (3), 184−187.
(77) Gabov, I.; Ezhikova, M.; Kodess, M.; Pestov, A. Effect of the structure of alkylammonium halides on the outcome of carbon dioxide cycloaddition to oxiranes. *Russ. Chem. Bull.* **2023**, *72* (12), 2809−2814.
(78) Saha, A.; Pal, A.; Mukherjee, D.; Pal, S. C.; Das, M. C. Two-Dimensional Cu (II)-MOF with Lewis Acid-Base Bifunctional Sites for Chemical Fixation of CO_2 and Bioactive 1,4-DHP Synthesis via Hantzsch Condensation. *Inorg. Chem.* **2024**, *63* (23), 10832−10842.
(79) Das, S.; Zhang, J.; Chamberlain, T. W.; Clarkson, G. J.; Walton, R. I. Nonredox CO_2 Fixation in Solvent-Free Conditions Using a Lewis Acid Metal-Organic Framework Constructed from a Sustainably Sourced Ligand. *Inorg. Chem.* **2022**, *61* (46), 18536−18544.
(80) Liu, M.; Liu, B.; Zhong, S.; Shi, L.; Liang, L.; Sun, J. Kinetics and Mechanistic Insight into Efficient Fixation of CO_2 to Epoxides over N-Heterocyclic Compound/$ZnBr_2$ Catalysts. *Ind. Eng. Chem. Res.* **2015**, *54* (2), 633−640.
(81) Abazari, R.; Ghorbani, N.; Shariati, J.; Varma, R. S.; Qian, J. Copper-Based Bio-MOF/GO with Lewis Basic Sites for CO_2 Fixation into Cyclic Carbonates and C−C Bond-Forming Reactions. *Inorg. Chem.* **2024**, *63* (27), 12667−12680.
(82) Fei, Y.; Abazari, R.; Ren, M.; Wang, X.; Zhang, X. Defect Engineering in a Nanoporous Thulium-Organic Framework in Catalyzing Knoevenagel Condensation and Chemical CO_2 Fixation. *Inorg. Chem.* **2024**, *63* (40), 18914−18923.
(83) Lin, J.-B.; Nguyen, T. T.; Vaidhyanathan, R.; Burner, J.; Taylor, J. M.; Durekova, H.; Akhtar, F.; Mah, R. K.; Ghaffari-Nik, O.; Marx, S.; et al. A scalable metal-organic framework as a durable physisorbent for carbon dioxide capture. *Science* **2021**, *374* (6574), 1464−1469.
(84) Kuruppathparambil, R. R.; Robert, T. M.; Pillai, R. S.; Pillai, S. K. B.; Kalamblayil Shankaranarayanan, S. K.; Kim, D.; Mathew, D. Nitrogen-rich dual linker MOF catalyst for room temperature fixation of CO_2 via cyclic carbonate synthesis: DFT assisted mechanistic study. *J. CO_2 Util.* **2022**, *59*, 101951.
(85) Fei, Y.; Abazari, R.; Ren, M.; Wang, X.; Zhang, X. Defect Engineering in a Nanoporous Thulium-Organic Framework in Catalyzing Knoevenagel Condensation and Chemical CO_2 Fixation. *Inorg. Chem.* **2024**, *63* (40), 18914−18923.
(86) Stubbs, A. W.; Braglia, L.; Borfecchia, E.; Meyer, R. J.; Román-Leshkov, Y.; Lamberti, C.; Dincă, M. Selective Catalytic Olefin Epoxidation with Mn^{II}-Exchanged MOF-5. *ACS Catal.* **2018**, *8* (1), 596−601.

https://doi.org/10.1021/acs.langmuir.5c00906
Langmuir 2025, 41, 19101−19110